

Article

Fabrication of Core-Shell Magnetic Molecularly Imprinted Nanospheres towards Hypericin via Click Polymerization

Xinxin Wang, Yuxin Pei *, Yong Hou and Zhichao Pei

Shaanxi Key Laboratory of Natural Products & Chemical Biology, College of Chemistry & Pharmacy, Northwest A&F University, Yangling 712100, Shaanxi, China; xinxinwang@nwafu.edu.cn (X.W.); yixilun@126.cn (Y.H.); peizc@nwafu.edu.cn (Z.P.)

* Correspondence: peiyx@nwafu.edu.cn; Tel.: +86-29-87091196; Fax: +86-29-87092769

Received: 6 January 2019; Accepted: 3 February 2019; Published: 13 February 2019



Abstract: The core-shell structure molecularly imprinted magnetic nanospheres towards hypericin ($\text{Fe}_3\text{O}_4\text{@MIPs}$) were prepared by mercapto-alkyne click polymerization. The shape and size of nanospheres were characterized by dynamic light scattering (DLS) and transmission electron microscope (TEM). The nanospheres were analyzed by FTIR spectroscopy to verify the thiol-yne click reaction in the presence or absence of hypericin. The Brunauer–Emmet–Teller (BET) method was used for measuring the average pore size, pore volume and surface area. The $\text{Fe}_3\text{O}_4\text{@MIPs}$ synthesized displayed a good adsorption capacity ($Q = 6.80 \mu\text{mol}\cdot\text{g}^{-1}$). In addition, so-prepared $\text{Fe}_3\text{O}_4\text{@MIPs}$ showed fast mass transfer rates and good reusability. The method established for fabrication of $\text{Fe}_3\text{O}_4\text{@MIPs}$ showed excellent reproducibility and has broad potential for the fabrication of other core-shell molecularly imprinted polymers (MIPs).

Keywords: surface molecular imprinting; hypericin; click polymerization; core-shell; magnetic nanospheres

1. Introduction

Molecularly imprinted polymers (MIPs), mimicking a principle similar to antibody–antigen recognition, are synthesized via polymerization to create specific binding sites with memory of the template molecules during the synthetic process of polymers [1]. Molecular imprinting techniques based on MIPs have successfully obtained many applications, including separation [2], solid phase extraction (SPE) [3], chromatography [4], sensors [5], catalysis [6], immunoassay [7], and drug delivery due to the strengths of MIPs [8–10], such as high chemical stability, high affinity with templates, and low costs [11].

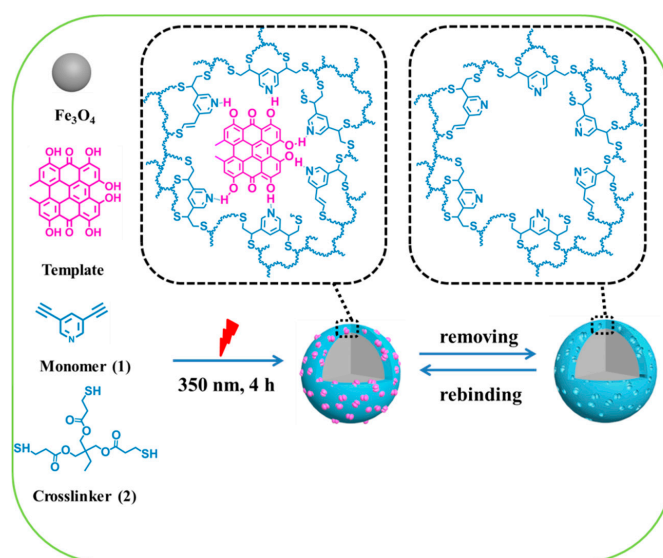
Commonly, MIPs were prepared by bulk polymerization, precipitation polymerization, and suspension polymerization. Bulky MIPs have the following shortcomings: (1) Inability to completely remove the template; (2) uneven distribution of binding sites; (3) a slow mass transfer rate; (4) and irregular resultant particle size and shape [12,13]. Surface molecularly imprinted polymers (SMIPs) based on core-shell nanoparticles have attracted considerable attention because they create recognition sites on a thin layer, and therefore significantly improve the mass transfer rate. Moreover, elution of templates from SMIPs is easier in comparison with bulky MIPs [14]. Consequently, various hard materials, including silica, graphene, gold–silver nanoparticles, and magnetic materials [15,16], were reported as cores in constructing core-shell MIPs via surface molecularly imprinting approaches. Among them, Fe_3O_4 magnetic nanoparticles (MNPs) are often used as cores for their numerous advantages, especially paramagnetic properties. Because the paramagnetic properties of MNPs allow

the final core-shell MIPs to be separated quickly and conveniently by a magnet in the separation process, they are highly desired in practical applications [17].

Hypericin (Hyp) has gained increasing interest from researchers due to its bioactivities, such as antidepressant [18], antiviral, antiseptic, antiphlogosis and antitumor properties [19–21]. However, extracting Hyp from St John's wort plant remains a challenge due to the low Hyp concentration of the plant and the shortage of specific adsorbents [22]. Our group has concentrated on fabricating specific adsorbents with high efficiency and high selectivity for Hyp in the past few years. For example, by using Fe_3O_4 as the core and polydopamine as the shell, we established a simple way to synthesize the core-shell magnetic molecularly imprinted nanosphere, which possesses great adsorption capacity ($Q = 18.28 \mu\text{mol}\cdot\text{g}^{-1}$) of Hyp. It also possesses obvious binding selectivity to Hyp [23]. However, the elution of Hyp was difficult due to the strong adsorption of Hyp on polydopamine (PDA).

Since the first report in 2001 [24], click reaction has been broadly applied in many fields such as polymer chemistry, functional materials, surface modification and biochemical sensors because of its high efficiency under mild conditions and fast kinetics. In contrast, only a few works have been published where fabrications of MIPs have been achieved through click reaction [25–28]. Previously, in order to obtain the polymeric nanospheres, we established a one-step method by using the click reaction between azide and alkyne with ultrasonic assistance in the absence of surfactants [29,30]. The size of the nanospheres could be controlled by using a different ratio of the rational designed monomers to crosslinkers and reaction conditions. Based on this work, we synthesized bulky MIP nanospheres by using tris (3-mercaptopropionate), 3,5-diethynyl-pyridine and Hyp (corresponding to crosslinker, monomer, and template, respectively) by mercapto-alkynyl click polymerization. The polymer nanospheres showed good capacity for adsorption and selectivity toward Hyp ($6.80 \mu\text{mol}\cdot\text{g}^{-1}$) [31]. Nevertheless, the separation of MIP nanospheres from the supernatant is difficult and needs a long duration of centrifugation on high speed, which limits their further practical application [32].

Based on our previous works [23,31], we envision that core-shell magnetic MIP nanospheres (denoted as $\text{Fe}_3\text{O}_4\text{@MIPs}$) can be fabricated by click polymerization between (1) 3,5-diethynyl-pyridine, and (2) tris (3-mercaptopropionate), on the surface of MNPs in the presence of Hyp. $\text{Fe}_3\text{O}_4\text{@MIPs}$ synthesized by this method should facilitate elution of the templates and separation of the nanospheres from the supernatant. Thus, $\text{Fe}_3\text{O}_4\text{@MIPs}$ were synthesized as depicted in Scheme 1 and evaluated accordingly in this work.



Scheme 1. Illustration for the preparation of core-shell structure molecularly imprinted magnetic nanospheres ($\text{Fe}_3\text{O}_4\text{@MIPs}$).

2. Materials and Methods

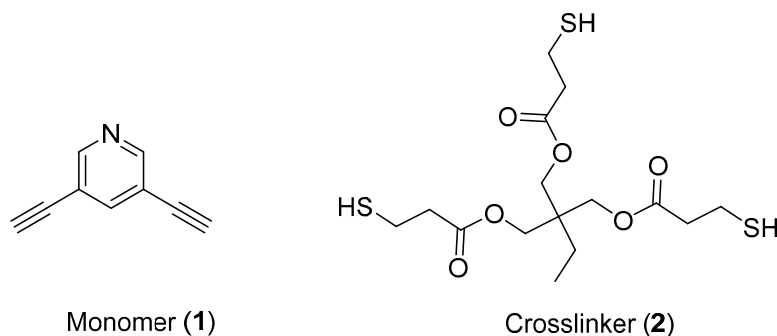
2.1. Materials

2-methyl-3-butyn-2-ol was obtained from J&K Scientific Ltd. Benzoin dimethyl ether (DMPA, 98%) was obtained from Tianjin Heowns Biochemical Technology Co., Ltd. (Tianjin, China). 3,5-dibromopyridine (98%), trimethylolpropane (>98%), copper (I) iodide (98%), sodium methylate (97%) and bis (triphenylphosphine) palladium (II) chloride (Pd 15.2%) were obtained from Aladdin (Shanghai, China). Emodin (Emo) was obtained from Tianfeng Biological Technology Co, Ltd. (Xi'an, China). Template molecules were synthesized on the basis of our previous work [33], and characterized by proton nuclear magnetic resonance ($^1\text{H-NMR}$). The other solvents and chemicals were analytical reagent (AR) grade and used as received without any further purification.

$^1\text{H-NMR}$ spectra were recorded on a Bruker AVANCEIII 500 MHz Spectrometer (Bruker, Fällanden, Switzerland). Transmission electron microscopy (TEM) was performed on an H-600 instrument by Hitachi Ltd. operating at 80 kV. Dynamic light scattering (DLS) (Beckman Coulter, Brea, CA, USA) was used to measure the hydrodynamic diameter of the particles. Nitrogen physisorption (Autosorb-iQ, Quantachrome, Boynton Beach, FL, USA) was used to measure the surface area and the porosity of the nanospheres. High performance liquid chromatography (HPLC): C18 reversed-phase column (5 μm , 4.6 mm \times 150 mm, Shimadzu, Kyoto, Japan).

2.2. Synthesis of Monomers and Crosslinkers

In this work, we used compounds **1** and **2** as monomers and crosslinkers for click polymerization (see Scheme 2). Compounds **1** and **2** were synthesized according to the published procedure [29,34] and characterized by $^1\text{H-NMR}$ (Bruker AVANCE III 500 MHz Spectrometer). The synthetic details can be found in Supplementary Materials and their $^1\text{H-NMR}$ spectra were shown in Figures S1, S2 and S6–S9.



Scheme 2. The chemical structures of the monomer (1) and the crosslinker (2).

2.3. Preparation of Fe_3O_4 MNPs

The Fe_3O_4 MNPs were prepared according to the published procedure [35]. $\text{FeCl}_3 \cdot 6\text{H}_2\text{O}$ (1.35 g, 5 mmol) was added to a beaker with 40 mL ethylene glycol, 1.0 g polyethylene glycol and 3.6 g NaAc. After being vigorously stirred for 30 min, the mixture was sealed in a stainless steel autoclave and kept at 200 $^\circ\text{C}$ for 10 h. Then, the mixture was cooled to room temperature to obtain MNPs. The MNPs were washed and stored in absolute ethanol.

2.4. Preparation of Core-Shell Molecularly Imprinted Polymer Magnetic Nanospheres towards Hyp (Fe_3O_4 @MIPs) via Click Reaction

The mixture containing MNPs (0.216 mmol), 0.1 mmol monomer **1**, 0.1 mmol crosslinker **2**, 0.031 mmol DMPA, 1.5 mL acetone, and 0.5 mL acetonitrile were placed into a quartz tube. The mixture was subjected to ultrasonication for 10 minutes before the addition of a 10 μmol template of Hyp. The final mixture was subjected to UV irradiation (350 nm) for click polymerization on the surface of

MNPs for 4 h at an ambient temperature under an inert atmosphere and mechanical stirring to yield Fe₃O₄@MIPs.

As shown in Figure 1, the final Fe₃O₄@MIPs were separated easily from the reaction system with a magnet, due to the paramagnetic property of MNPs, and extracted with acetone containing 10% acetic acid for 48 h in a Soxhlet apparatus, then subjected to ultrasonication in acetone containing 20% acetic acid for 20 min. The ultrasonication step was repeated until no Hyp was detected in the solvent.

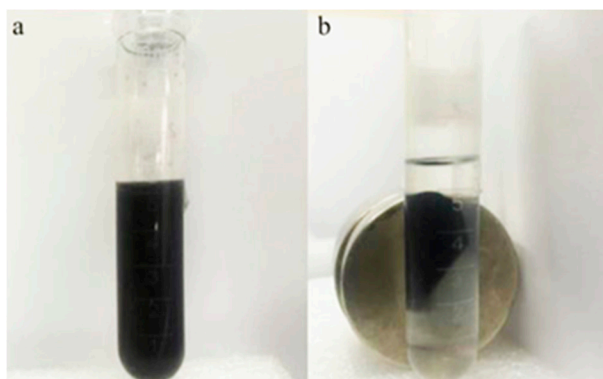


Figure 1. The photos of a suspension of Fe₃O₄@MIPs (a) and separation by magnets (b).

The same method was used for preparing the control polymer nanospheres (Fe₃O₄@NIPs) in the absence of the template molecules.

2.5. Determination of Static Adsorption Capacity

To obtain static adsorption capacity, a test molecule solution in acetone (5 mL, 1.0 μM) and 5 mg Fe₃O₄@MIPs (or Fe₃O₄@NIPs) were placed into 10 mL centrifuge tubes at 25 °C for 24 h, respectively. HPLC (C18 reversed-phase column, 5 μm, 4.6 mm × 150 mm) was used to measure the free test molecules in the supernatant (Figure S3). The adsorption capacity (Q , μmol·g⁻¹) was calculated using Equation (1):

$$Q = \frac{(C_0 - C_e) V}{W} \quad (1)$$

where C_e (μM) and C_0 (μM) are the equilibrium and the initial concentration; V (L) is the volume of the solution; and W (g) is the dry weight of the nanospheres.

The specific adsorption capacity (Q_s) of Fe₃O₄@MIPs is defined as Equation (2):

$$Q_s = Q_1 - Q_2 \quad (2)$$

where Q_1 (μmol·g⁻¹) and Q_2 (μmol·g⁻¹) are the static adsorption capacity of Fe₃O₄@MIPs and Fe₃O₄@NIPs, respectively.

2.6. Dynamic Adsorption Test

Fe₃O₄@MIPs or Fe₃O₄@NIPs (5.0 mg) were added into a centrifuge tube (10 mL). Hyp acetone solution (12.5 μM, 5 mL) was then placed into the tube. There after the tube was wrapped with aluminum foil and shaken in an air bath shaker at 25 °C for different lengths of time (0.5, 1, 2, 4, 8, and 12 h). HPLC was used to measure the concentrations of free Hyp in the supernatants, and each adsorption was calculated using Equation (1).

2.7. Isotherm Adsorption

The nanospheres (5.0 mg) were weighted into six centrifuge tubes with the Hyp acetone solution (5 mL). The concentrations of Hyp acetone solution were 2.5, 5.0, 10.0, 12.5, 25, and 50.0 μM, respectively.

Subsequently, the mixtures were shaken at 25 °C for 8 h. HPLC was used to measure the concentrations of Hyp in the supernatants. Each adsorption was then calculated using Equation (1).

2.8. Selectivity of Fe_3O_4 @MIPs and Fe_3O_4 @NIPs for Hyp

The binding selectivity of the nanospheres was studied according to the following method [23]. Briefly, Hyp, Protohyp, and Emo acetone solution (5 mL, 12.5 μ M) were incubated with 5 mg Fe_3O_4 @MIPs or Fe_3O_4 @NIPs at 25 °C for 24 h, respectively. The amounts of test molecules bound to the nanospheres were measured by HPLC. The “selectivity factor” (SF) and “imprinting factor” (IF) were used to compare the binding selectivity of the nanospheres [32], which can be defined by Equations (3) and (4), respectively:

$$D = \frac{C_0 - C_e}{C_e} \quad (3)$$

$$SF = \frac{D_{MIP}^h}{D'_{MIP}} = \frac{(C_{0, MIP}^h - C_{e, MIP}^h) / C_{e, MIP}^h}{(C'_{0, MIP} - C'_{e, MIP}) / C'_{e, MIP}}$$

where the distribution of hypericin for MIP ($L \cdot g^{-1}$) is represented as D_{MIP}^h , the distribution of competitor for MIP ($L \cdot g^{-1}$) is represented as D'_{MIP} , C_0 (μ M) is the initial concentration of hypericin, and C_e (μ M) is the concentration of hypericin after imprinted.

$$IF = \frac{D_{MIP}}{D_{NIP}} = \frac{(C_{0, MIP} - C_{e, MIP}) / C_{e, MIP}}{(C_{0, NIP} - C_{e, NIP}) / C_{e, NIP}} \quad (4)$$

where the distribution of the test molecule for MIP ($L \cdot g^{-1}$) is represented as D_{MIP} , the distribution of the test molecule for NIP ($L \cdot g^{-1}$) is represented as D_{NIP} , C_0 (μ M) is the initial concentration of hypericin, and C_e (μ M) is the concentration of hypericin after imprinted.

2.9. The Reusability of Fe_3O_4 @MIPs

Reusability was measured by following the previous report [23]. Fe_3O_4 @MIPs (5 mg) and Hyp of acetone solution (5 mL, 12.5 μ M) were mixed at 25 °C and the mixtures were shaken for 8 h. Following this, HPLC was used for measuring the concentration of Hyp in the supernatant. The adsorption capacity was calculated by Equation (1).

2.10. Brunauer–Emmet–Teller Analysis

The average pore size, pore volume and surface area of the nanospheres were analyzed by Autosorb-iQ nitrogen physisorption made by Quantachrome, based on the Brunauer–Emmet–Teller (BET) method. Prior to analysis, the samples were placed into vacuum drying oven at 50 °C for 9 h.

2.11. HPLC Analysis

The solution of herb extract was prepared by following a previously reported method [23]. The herb extract solution (8 mL) was mixed with Hyp acetone solution (1 mL, 125 μ M) and Protohyp acetone solution (1 mL, 125 μ M) to obtain an original solution. 5 mL of this solution was mixed with 5 mg of the nanospheres (Fe_3O_4 @MIPs or Fe_3O_4 @NIPs) and shaken for 8 h. The concentration of each compound in the supernatant was measured by HPLC [31].

3. Results and Discussion

3.1. Preparation of Fe_3O_4 @MIPs

Fe_3O_4 @MIPs were synthesized according to the procedure described in Scheme 1. MNPs, compound 1, and compound 2, were mixed and dealt with ultrasound for 10 min before the template

was added. The final mixture was then irradiated by a UV light of 350 nm to initiate the click polymerization on the surface of MNPs. The imprinting sites were created due to the formation of the complex between the template and monomer via π - π interaction, hydrogen bonds and sequential click polymerization. For obtaining the Fe_3O_4 @MIPs, Hyp molecules were removed.

3.2. Characterization of Fe_3O_4 @MIPs

3.2.1. FTIR Analysis

The shell of magnetic nanospheres was analyzed by FTIR spectroscopy to verify the thiol-yne click reaction in the presence or absence of Hyp. Their IR spectra, along with those of monomer **1**, crosslinker **2**, Hyp, and MNPs, are shown in Figure 2. It can be seen that, neither characteristic absorptions at 2103 and 3274 cm^{-1} ($\text{C}\equiv\text{C}$ and $\text{C}-\text{H}$ in alkynyl groups) on monomer **1** [29], nor characteristic absorptions at 1735 and 2570 cm^{-1} ($\text{C}=\text{O}$ and $\text{S}-\text{H}$) on crosslinker **2** were observed on both spectra of Fe_3O_4 @MIPs and Fe_3O_4 @NIPs. In addition, the absorption band of $\text{C}-\text{O}$ on Hyp at 1230 cm^{-1} [23] was found on the spectrum of Fe_3O_4 @MIPs, but not on that of Fe_3O_4 @NIPs. All these indicated that the thiol-yne click reaction successfully occurred in the presence and absence of Hyp.

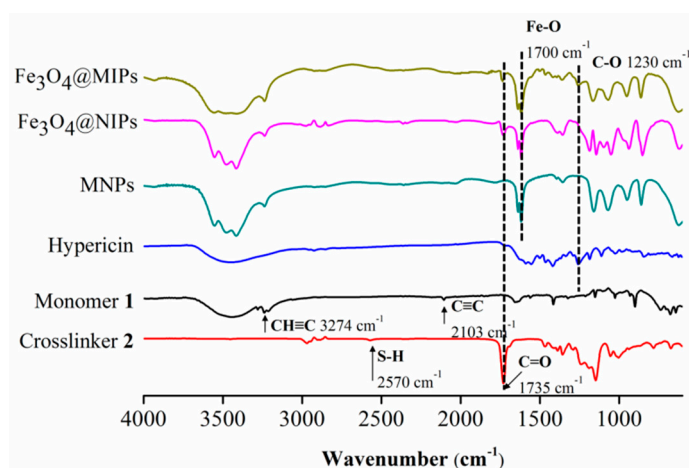


Figure 2. FTIR spectra of Fe_3O_4 @MIPs, Fe_3O_4 @NIPs, MNPs, Hyp, monomer **1**, and crosslinker **2**.

3.2.2. Morphological Features

Size and morphology of MNPs, Fe_3O_4 @NIPs and Fe_3O_4 @MIPs were characterized by H-600 TEM (Hitachi Ltd.) and DLS (Beckman Coulter). Their TEM images are displayed in Figure 3. It can be seen that the original spherical shape of MNPs were kept in the resulting Fe_3O_4 @MIPs and Fe_3O_4 @NIPs. Compared to MNPs, a light gray layer around MNPs was observed in both scenarios, which indicated the shell was formed on the surface of the MNPs via click polymerization.

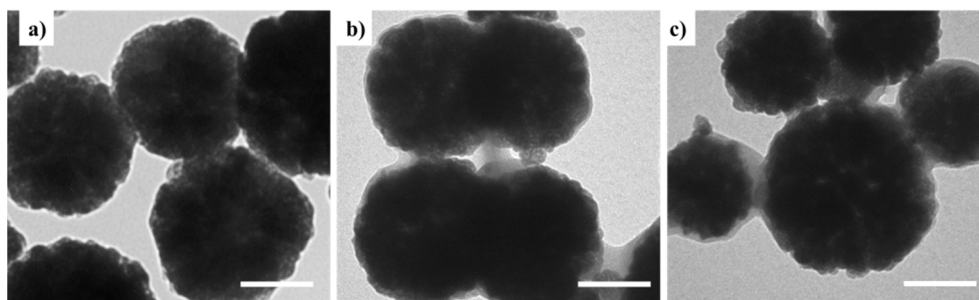


Figure 3. TEM images of MNPs (a), Fe_3O_4 @MIPs (b), and Fe_3O_4 @NIPs (c). Scale bar: 100 nm.

DLS analysis (Figure S4 and Table 1) showed that the average hydrodynamic diameters of Fe₃O₄@MIPs and Fe₃O₄@NIPs are 344 and 320 nm, respectively, which is an increase of 35 and 11 nm, respectively, in comparison with that of MNPs (309 nm). The increase of the diameters was due to the formation of a polymer film on the surface of MNPs. The thicker polymer layer of Fe₃O₄@MIPs was attributed to the presence of Hyp during polymerization which resulted in the formation of a porous polymer film. The polydispersity indexes of Fe₃O₄@MIPs and Fe₃O₄@NIPs were 0.386 and 0.315, respectively. Notably, the ζ potential of Fe₃O₄@MIPs was changed from 3.49 to -3.58 mV during the extraction process; while the ζ potential of Fe₃O₄@NIPs was not affected significantly. The results were consistent with those previously reported [23,31]. This was due to the removal of Hyp molecules from the Fe₃O₄@MIPs nanospheres. The result confirms that the Fe₃O₄@MIPs can be established by click polymerization between **1** and **2**.

Table 1. Dynamic light scattering (DLS) and Zeta data of the nanospheres prepared.

Nanospheres	Particle Size (nm)	Polydispersity Index	ζ Potential (mV)
MNPs	309 \pm 61	0.271	1.35 \pm 0.17
Fe ₃ O ₄ @MIPs	344 \pm 55	0.386	3.49 \pm 0.72
Fe ₃ O ₄ @NIPs	320 \pm 75	0.315	2.06 \pm 0.86
Fe ₃ O ₄ @MIPs after extracting process	323 \pm 80	0.646	-3.58 ± 0.58
Fe ₃ O ₄ @NIPs after extracting process	314 \pm 46	0.378	0.20 \pm 0.69

3.2.3. BET Analysis

The BET method was used to measure the average pore size, pore volume and surface area of Fe₃O₄@MIPs and Fe₃O₄@NIPs (Table 2, Figure S5). The average pore size of Fe₃O₄@MIPs is 19.18 nm, nearly 2.5 times higher than that of the Fe₃O₄@NIPs, and the surface area and pore volume of Fe₃O₄@MIPs are 8.31 m²·g⁻¹ and 0.04 cm³·g⁻¹, respectively; which is nearly three times and 10 times higher than that of Fe₃O₄@NIPs, respectively. This indicates that the imprinted polymer layer has a porous structure; in contrast, the non-imprinted polymer layer is relatively dense.

Table 2. Pore size, surface area, and pore volume of nanospheres.

Nanospheres	Average Pore Diameter (nm)	Surface Area (m ² ·g ⁻¹)	Pore Volume (cm ³ ·g ⁻¹)
Fe ₃ O ₄ @MIPs	19.18 \pm 0.26	8.31 \pm 0.25	0.04 \pm 0.03
Fe ₃ O ₄ @NIPs	7.84 \pm 0.12	2.81 \pm 0.01	0.004 \pm 0.01

3.3. Dynamic Adsorption Study

Dynamic adsorption of Fe₃O₄@MIPs and Fe₃O₄@NIPs were studied. As shown in Figure 4, adsorption amount increased rapidly with time, and reached about 90% at 4 h, which indicates that the Fe₃O₄@MIPs obtained good mass transfer properties and that the template molecules reached surface recognition sites relatively easily. Following on from this period, the prolongation of incubation time did not lead to an obvious increase of adsorption. For instance, it took another 4 h to reach the remaining 10% of the total adsorption capacity (equilibrium). While the adsorption amount of Fe₃O₄@NIPs towards Hyp under the same conditions, driven by non-specific interaction between the template and the polymer surface, was lower than that of Fe₃O₄@MIPs. This was due to the absence of specific recognition sites, small pore volume and low surface area of the Fe₃O₄@NIPs.

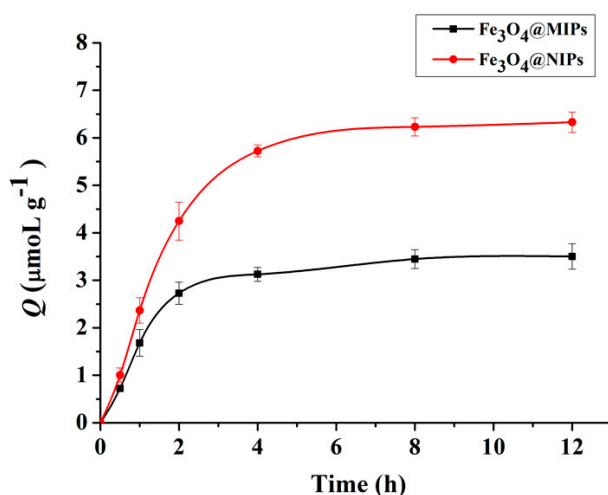


Figure 4. Dynamic adsorption curves of Hyp on $\text{Fe}_3\text{O}_4\text{@MIPs}$ and $\text{Fe}_3\text{O}_4\text{@NIPs}$ ($n = 3$).

3.4. Affinity Analysis

The ability of $\text{Fe}_3\text{O}_4\text{@MIPs}$ for Hyp specific recognition was studied by way of an isothermal adsorption experiment with different concentrations of Hyp (0–50.0 μM). The Q values of $\text{Fe}_3\text{O}_4\text{@MIPs}$ and $\text{Fe}_3\text{O}_4\text{@NIPs}$ are shown in Figure 5a. It can be seen that the binding amount of $\text{Fe}_3\text{O}_4\text{@MIPs}$ increased rapidly in a linear relationship with the concentration of Hyp when it was lower than C_s (11.91 μM). When the concentration reached C_s , the adsorption of $\text{Fe}_3\text{O}_4\text{@MIPs}$ reached equilibrium (Q_{max}) at $6.33 \mu\text{mol}\cdot\text{g}^{-1}$, which is much higher than that obtained with $\text{Fe}_3\text{O}_4\text{@NIPs}$ under the same conditions, and can be ascribed to the imprinting effect [22]. Notably, the value of C_s is very close to the one reported previously for bulk MIP nanospheres fabricated via the same click polymerization [31]. This indicates that the property of the polymer film on the surface of so-prepared core-shell $\text{Fe}_3\text{O}_4\text{@MIPs}$ is well kept.

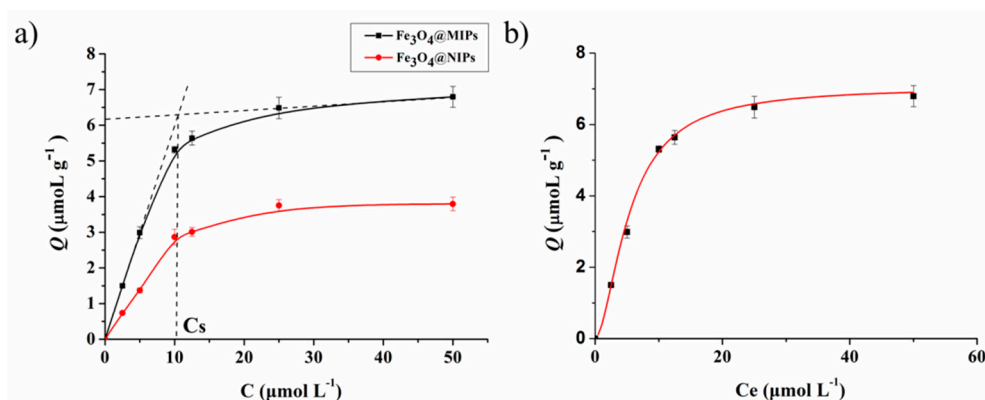


Figure 5. (a) The isothermal adsorption curve of $\text{Fe}_3\text{O}_4\text{@MIPs}$ and $\text{Fe}_3\text{O}_4\text{@NIPs}$; (b) the fitting curve of the extended Langmuir adsorption ($n = 3$).

The adsorption mechanism was studied by plotting the equilibrium concentrations of Hyp against the corresponding amounts of Hyp bound to $\text{Fe}_3\text{O}_4\text{@MIPs}$. As shown in Figure 5b, it fitted well with the extended model of Langmuir adsorption isotherm expressed by Equation (5) [22,36], where R^2 is 0.9964, $K_d = 0.0552 \mu\text{M}$, m is 1.7052, and Q_{max} is $7.0524 \mu\text{mol}\cdot\text{g}^{-1}$. The result proved that the adsorption was monolayer adsorption on a non-smooth surface.

$$\frac{C_e^m}{Q} = \frac{1}{K_d Q_{max}} + \frac{C_e^m}{Q_{max}} \quad (5)$$

where C_e ($\mu\text{mol}\cdot\text{L}^{-1}$) is equilibrium concentration of Hyp in the supernatant, K_d (μM) is the equilibrium constant, and Q_{max} ($\mu\text{mol}\cdot\text{g}^{-1}$) is the maximum adsorption capacity of binding sites.

3.5. Binding Selectivity of Fe_3O_4 @MIPs to the Template Molecule Hyp

The binding selectivity of Fe_3O_4 @MIPs to the template molecule Hyp was measured by a similar method, described in our previous work [23]. Briefly, two phenolic compounds containing phenolic hydroxyl groups, Protohyp and Emo (with chemical structures shown in Figure 6a), were selected as the competitors of Hyp. The respective adsorption capacities of Fe_3O_4 @MIPs and Fe_3O_4 @NIPs towards Hyp, Protohyp, and Emo were measured under the same conditions. The results are shown in Figure 6b. The adsorption of Fe_3O_4 @MIPs towards Hyp was clearly much higher than Protohyp and Emo. In contrast, the respective adsorptions of Fe_3O_4 @NIPs toward the three different molecules remained similar.

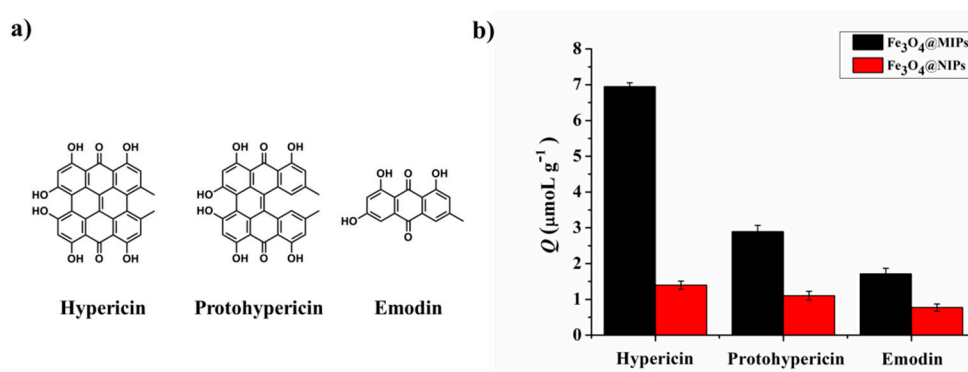


Figure 6. Competitive experiment of Hyp and Hyp structure analogues ($n = 3$).

SF and IF were used to evaluate the binding selectivity of the nanospheres (Table 3). The SF of Fe_3O_4 @MIPs for Protohyp and Emo were 4.16 and 7.88, respectively. The IF of Fe_3O_4 @MIPs towards Hyp, Protohyp, and Emo was 9.93, 3.11, and 2.41, respectively.

Table 3. The values of SF and IF.

Factor	Hyp	Protohyp	Emodin
SF	-	4.16	7.88
IF	9.93	3.11	2.41

3.6. Reproducibility and Reusability of Fe_3O_4 @MIPs

To test the reproducibility of the method in preparing Fe_3O_4 @MIPs, three parallel experiments were conducted, the products were subjected to adsorption capacity evaluation under the same conditions. As shown in Figure 7, similar adsorption capacities for each individually prepared Fe_3O_4 @MIPs were obtained (6.80, 6.65, and 6.56 $\mu\text{mol}\cdot\text{g}^{-1}$, respectively). The results showed that the click polymerization method used to fabricate Fe_3O_4 @MIPs was reproducible and that nanospheres can be used for selective identification of Hyp.

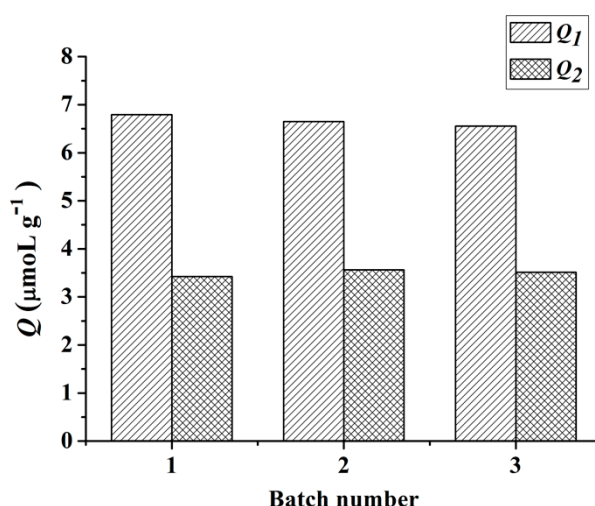


Figure 7. Reproducibility of the method for preparing Fe_3O_4 @MIPs.

As a man-made antibody, one of the numerous advantages of MIPs in comparison with native antibodies, is the robustness of the materials which allows for repeated use [37]. Therefore, the reusability of Fe_3O_4 @MIPs was evaluated and the results are shown in Figure 8. As expected, we found that the adsorption capacity of Fe_3O_4 @MIPs, similar to its bulky counterpart [31], changed little even after five adsorption–extraction cycles, indicating that nanospheres of Fe_3O_4 @MIPs have good stability.

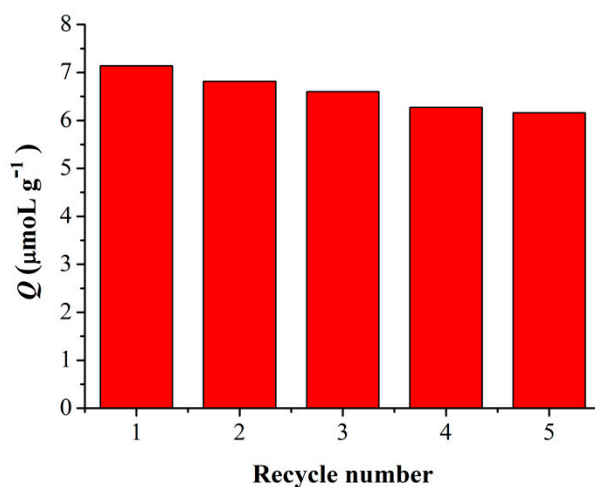


Figure 8. Reusability of Fe_3O_4 @MIPs.

3.7. Adsorption of Fe_3O_4 @MIPs toward Hyp from the Herb Extract

Adsorption of Fe_3O_4 @MIPs from the herb extract was investigated using a published procedure [23]. To measure selective adsorption ability of Fe_3O_4 @MIPs towards Hyp, the herb extract was mixed with Hyp and Protohyp (equal amounts). HPLC was used to measure the concentration of Hyp in the supernatant, and the results are shown in Figure 9 and Table 4. As shown in Figure 9, the peaks of Protohyp and Hyp were found. As can be seen in Table 4, 46.5% of Hyp was adsorbed by Fe_3O_4 @MIPs, while 18.6% was adsorbed by Fe_3O_4 @NIPs. Here, Fe_3O_4 @MIPs showed 2.5 times higher adsorption than Fe_3O_4 @NIPs toward Hyp. However, there was no obvious difference observed for the adsorption of Fe_3O_4 @NIPs towards Hyp and Protohyp (18.6% and 20.3%, respectively), nor for the adsorption of Fe_3O_4 @NIPs and Fe_3O_4 @MIPs towards non-template molecules of Protohyp (20.3% and 21.5%, respectively), which implied that the adsorption was non-specific.

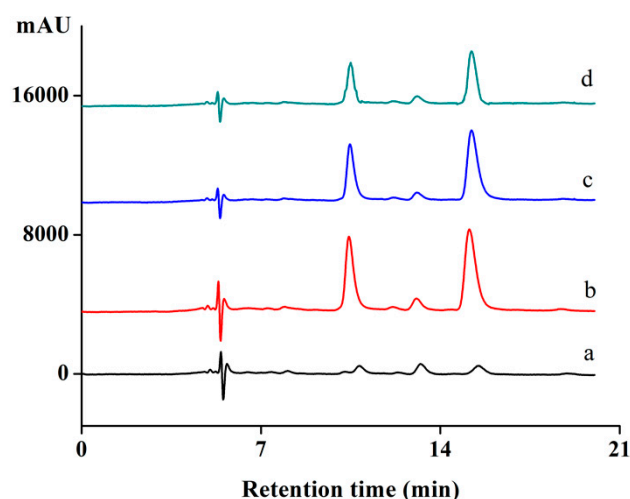


Figure 9. Chromatograms of (a) herb extract; (b) mixture of extract, Hyp and Protohyp (before adsorption); (c) supernatant of Fe_3O_4 @NIPs (after adsorption); (d) supernatant of Fe_3O_4 @MIPs (after adsorption).

Table 4. Adsorption capacity of nanospheres for extracts.

Sample	Peak Area (Hyp)	Peak Area (Protohyp)	Adsorption of Hyp (%)	Adsorption of Protohyp (%)
Initial	141,375	80,769	-	-
Fe_3O_4 @NIPs	115,094	64,398	18.6	20.3
Fe_3O_4 @MIPs	75,618	63,397	46.5	21.5

4. Conclusions

In conclusion, Fe_3O_4 @MIPs with core-shell structures were prepared by mercapto-alkyne click polymerization. The Fe_3O_4 @MIPs showed good specific adsorption towards Hyp and easy separation properties. In addition, Fe_3O_4 @MIPs showed fast mass transfer rates, good reusability and had potential application in enriching and separating Hyp from herb extracts. Most importantly, this work opens an avenue for the fabrication of core-shell MIPs using click polymerization. Furthermore, MIPs prepared in this method may find potential applications in enrichment, rapid separation, and purification of Hypericin.

Supplementary Materials: The following are available online at <http://www.mdpi.com/2073-4360/11/2/313/s1>. Figure S1. The Synthesis of monomer **1**; Figure S2. The Synthesis of crosslinker **2**; Figure S3. (a) Standard curve of Hyp in acetone by HPLC. (b) Standard curve of Protohyp in acetone by HPLC. (c) Standard curve of emodin in acetone by HPLC. HPLC detection conditions: C18 reversed-phase column (5 μm , 4.6 mm \times 250 mm, Shimadzu, Japan). The mobile phase consisted of 50% acetonitrile, 50% of the mixture of ammonium acetate-acetic acid buffer (0.3 M, pH = 6.96) and methanol (1:4, v/v); detection wavelength: 590 nm; flow rate: 0.4 mL/min; injection volume: 10 μL ; Figure S4. DLS histograms of Fe_3O_4 @MIPs and Fe_3O_4 @NIPs before and after extracting process; Figure S5. The nitrogen adsorption and desorption isotherms of Fe_3O_4 @MIPs and Fe_3O_4 @NIPs; Figure S6. The $^1\text{H-NMR}$ spectrum of the monomer **1**; Figure S7. The $^1\text{H-NMR}$ spectrum of crosslinker **2**; Figure S8. The $^1\text{H-NMR}$ spectrum of Protohyp; Figure S9. The $^1\text{H-NMR}$ spectrum of Hyp.

Author Contributions: X.W. performed experiments, analyzed data and assisted in drafting the manuscript. Y.P. directed the entire research work and drafted the manuscript. Y.H. performed experiments. Z.P. assisted with discussion and revision of the manuscript.

Funding: This research was funded by the National Natural Science Foundation of China (21772157 and 21572181) and the Project of Science and Technology of Social Development in Yangling Demonstration Zone (2017SF-02).

Conflicts of Interest: The authors declare no conflicts of interest.

References

1. Mosbach, K.; Ramstrom, O. The emerging technique of molecular imprinting and its future impact on biotechnology. *Bio-Technol.* **1996**, *14*, 163–170. [[CrossRef](#)]
2. Li, P.F.; Wang, T.; Lei, F.H.; Peng, X.Y.; Wang, H.Y.; Qin, L.T.; Jiang, J.X. Preparation and evaluation of paclitaxel-imprinted polymers with a rosin-based crosslinker as the stationary phase in high-performance liquid chromatography. *J. Chromatogr. A* **2017**, *1502*, 30–37. [[CrossRef](#)] [[PubMed](#)]
3. Walshe, M.; Howarth, J.; Kelly, M.T.; OKennedy, R.; Smyth, M.R. The preparation of a molecular imprinted polymer to 7-hydroxycoumarin and its use as a solid-phase extraction material. *J. Pharmaceut. Biomed.* **1997**, *16*, 319–325. [[CrossRef](#)]
4. Sun, G.Y.; Liu, Y.F.; Ahat, H.J.; Shen, A.; Liang, X.M.; Xue, X.Y.; Luo, Y.Q.; Yang, P.; Liu, Z.S.; Aisa, H.A. “Two-dimensional” molecularly imprinted solid-phase extraction coupled with crystallization and high performance liquid chromatography for fast semi-preparative purification of tannins from pomegranate husk extract. *J. Chromatogr. A* **2017**, *1505*, 35–42. [[CrossRef](#)] [[PubMed](#)]
5. Piletsky, S.A.; Parhometz, Y.P.; Lavryk, N.V.; Panasyuk, T.L.; Elskaya, A.V. Sensors for low-weight organic-molecules based on molecular imprinting technique. *Sens. Actuat. B-Chem.* **1994**, *19*, 629–631. [[CrossRef](#)]
6. Guo, Y.; Guo, T.Y. A dual-template imprinted capsule with remarkably enhanced catalytic activity for pesticide degradation and elimination simultaneously. *Chem. Commun.* **2013**, *49*, 1073–1075. [[CrossRef](#)]
7. Muldoon, M.T.; Stanker, L.H. Application of molecularly-imprinted polymers for rapid sample cleanup: Immunochemical and HPLC analysis. *Arab. J. Sci. Eng.* **2014**, *39*, 2561–2572.
8. Norell, M.C.; Andersson, H.S.; Nicholls, I.A. Theophylline molecularly imprinted polymer dissociation kinetics: A novel sustained release drug dosage mechanism. *J. Mol. Recognit.* **1998**, *11*, 98–102. [[CrossRef](#)]
9. Alvarez-Lorenzo, C.; Concheiro, A. Molecularly imprinted polymers for drug delivery. *J. Chromatogr. B* **2004**, *804*, 231–245. [[CrossRef](#)]
10. Cunliffe, D.; Kirby, A.; Alexander, C. Molecularly imprinted drug delivery systems. *Adv. Drug. Deliver. Rev.* **2005**, *57*, 1836–1853. [[CrossRef](#)]
11. Pardeshi, S.; Singh, S.K. Precipitation polymerization: A versatile tool for preparing molecularly imprinted polymer beads for chromatography applications. *RSC Adv.* **2016**, *6*, 23525–23536. [[CrossRef](#)]
12. Cederfur, J.; Pei, Y.X.; Meng, Z.H.; Kempe, M. Synthesis and screening of a molecularly imprinted polymer library targeted for penicillin g. *J. Comb. Chem.* **2003**, *5*, 67–72. [[CrossRef](#)] [[PubMed](#)]
13. Zhang, Z.L.; Niu, D.C.; Li, Y.S.; Shi, J.L. Magnetic, core-shell structured and surface molecularly imprinted polymers for the rapid and selective recognition of salicylic acid from aqueous solutions. *Appl. Surf. Sci.* **2018**, *435*, 178–186. [[CrossRef](#)]
14. Gu, X.H.; Xu, R.; Yuan, G.L.; Lu, H.; Gu, B.R.; Xie, H.P. Preparation of chlorogenic acid surface-imprinted magnetic nanoparticles and their usage in separation of traditional chinese medicine. *Anal. Chim. Acta* **2010**, *675*, 64–70. [[CrossRef](#)] [[PubMed](#)]
15. Ozcan, A.A.; Ersoz, A.; Hur, D.; Yilmaz, F.; Gultekin, A.; Denizli, A.; Say, R. Semi-synthetic biotin imprinting onto avidin crosslinked gold-silver nanoparticles. *J. Nanopart. Res.* **2012**, *14*, 945. [[CrossRef](#)]
16. Ma, J.; Yuan, L.H.; Ding, M.J.; Wang, S.; Ren, F.; Zhang, J.; Du, S.H.; Li, F.; Zhou, X.M. The study of core-shell molecularly imprinted polymers of 17 beta-estradiol on the surface of silica nanoparticles. *Biosens. Bioelectron.* **2011**, *26*, 2791–2795. [[CrossRef](#)] [[PubMed](#)]
17. Machynakova, A.; Hrobonova, K. Preparation and application of magnetic molecularly imprinted polymers for the selective extraction of coumarins from food and plant samples. *Anal. Methods-UK* **2017**, *9*, 2168–2176. [[CrossRef](#)]
18. Harrer, G.; Sommer, H. Treatment of mild/moderate depressions with Hypericum. *Phytomed. Int. J. Phytother. Phytopharm.* **1994**, *1*, 3–8. [[CrossRef](#)]
19. Asgarpanah, J. Phytochemistry, pharmacology and medicinal properties of *Hypericum perforatum* L. *Afr. J. Pharm. Pharmacol.* **2012**, *6*, 1387–1394. [[CrossRef](#)]
20. Yip, L.; Hudson, J.B.; GruszeckaKowalik, E.; Zalkow, L.H.; Towers, G.H.N. Antiviral activity of a derivative of the photosensitive compound hypericin. *Phytomedicine* **1996**, *3*, 185–190. [[CrossRef](#)]
21. Stojanovic, G.; Dordevic, A.; Smelcerovic, A. Do other hypericum species have medical potential as St. John’s wort (*Hypericum perforatum*)? *Curr. Med. Chem.* **2013**, *20*, 2273–2295. [[CrossRef](#)] [[PubMed](#)]

22. Li, Z.Z.; Qin, C.L.; Li, D.M.; Hou, Y.Z.; Li, S.B.; Sun, J.J. Molecularly imprinted polymer for specific extraction of hypericin from *Hypericum perforatum* L. Herbal extract. *J. Pharmaceut. Biomed.* **2014**, *98*, 210–220. [[CrossRef](#)] [[PubMed](#)]
23. Cheng, W.X.; Fan, F.F.; Zhang, Y.; Pei, Z.C.; Wang, W.J.; Pei, Y.X. A facile approach for fabrication of core-shell magnetic molecularly imprinted nanospheres towards hypericin. *Polymers* **2017**, *9*, 135. [[CrossRef](#)]
24. Kolb, H.C.; Finn, M.G.; Sharpless, K.B. Click chemistry: Diverse chemical function from a few good reactions. *Angew. Chem. Int. Ed.* **2001**, *40*, 2004–2021. [[CrossRef](#)]
25. Xu, C.G.; Shen, X.T.; Ye, L. Molecularly imprinted magnetic materials prepared from modular and clickable nanoparticles. *J. Mater. Chem.* **2012**, *22*, 7427–7433. [[CrossRef](#)]
26. Stephenson-Brown, A.; Acton, A.L.; Preece, J.A.; Fossey, J.S.; Mendes, P.M. Selective glycoprotein detection through covalent templating and allosteric click-imprinting. *Chem. Sci.* **2015**, *6*, 5114–5119. [[CrossRef](#)] [[PubMed](#)]
27. Xu, Z.F.; Deng, P.H.; Tang, S.P.; Kuang, D.Z. Preparation of 2D molecularly imprinted materials based on mesoporous silicas via click reaction. *J. Mater. Chem. B* **2014**, *2*, 8418–8426. [[CrossRef](#)]
28. Zhao, T.; Wang, J.P.; He, J.L.; Deng, Q.L.; Wang, S. One-step post-imprint modification achieve dual-function of glycoprotein fluorescent sensor by “click chemistry”. *Biosens. Bioelectron.* **2017**, *91*, 756–761. [[CrossRef](#)]
29. Hou, Y.; Cao, S.P.; Li, X.M.; Wang, B.B.; Pei, Y.X.; Wang, L.; Pei, Z.C. One-step synthesis of dual clickable nanospheres via ultrasonic-assisted click polymerization for biological applications. *Appl. Mater. Inter.* **2014**, *6*, 16909–16917. [[CrossRef](#)]
30. Hou, Y.; Cao, S.P.; Wang, L.; Pei, Y.X.; Zhang, G.Y.; Zhang, S.W.; Pei, Z.C. Morphology-controlled dual clickable nanoparticles via ultrasonic-assisted click polymerization. *Polym. Chem.-UK* **2015**, *6*, 223–227. [[CrossRef](#)]
31. Pei, Y.X.; Fan, F.F.; Wang, X.X.; Feng, W.W.; Hou, Y.; Pei, Z.C. Fabrication of hypericin imprinted polymer nanospheres via thiol-yne click reaction. *Polymers* **2017**, *9*, 469. [[CrossRef](#)]
32. Ansell, R.J. Characterization of the Binding Properties of Molecularly Imprinted Polymers. *Adv. Biochem. Eng. Biotechnol.* **2015**, *150*, 51–93. [[PubMed](#)]
33. Zhang, Y.; Shang, K.; Wu, X.W.; Song, S.Y.; Li, Z.B.; Pei, Z.C.; Pei, Y.X. Highly efficient green synthesis and photodynamic therapeutic study of hypericin and its derivatives. *RSC Adv.* **2018**, *8*, 21786–21792. [[CrossRef](#)]
34. Jin, F.; Zheng, M.L.; Zhang, M.L.; Zhao, Z.S.; Duan, X.M. A facile layer-by-layer assembly method for the fabrication of fluorescent polymer/quantum dot nanocomposite thin films. *RSC Adv.* **2014**, *4*, 33206–33214. [[CrossRef](#)]
35. Deng, H.; Li, X.L.; Peng, Q.; Wang, X.; Chen, J.P.; Li, Y.D. Monodisperse magnetic single-crystal ferrite microspheres. *Angew. Chem. Int. Ed.* **2010**, *44*, 2782–2785. [[CrossRef](#)] [[PubMed](#)]
36. Senhadjikebiche, O.; Belaid, T.; Benamor, M. Preparation and characterization of molecularly imprinted polymer as spe sorbent for melamine isolation. *Polymers* **2013**, *5*, 1215–1228.
37. Kupai, J.; Rojik, E.; Huszthy, P.; Szekely, G. Role of chirality and macroring in imprinted polymers with nantiodiscriminative power. *Appl. Mater. Interfaces* **2015**, *7*, 9516–9952. [[CrossRef](#)]

